A HETEROGENEOUS DATASETS IN THE LITERATURE

We list the heterogeneous datasets used in the literature in the past six years in the following table.

Table 5: A survey of the existing heterogeneous graph data sets ("B":billion;"M":million;"K":thousand).

Year	Paper	Dataset	# Node	# Edge	# Edge/# Node
2015	HNE (2015) [7]	BlogCatalog	5,196	171,743	33.05
2017	MVE [36]	PPI	16,545	1,098,711	66.41
		DBLP	69,110	1,884,236	27.26
		Youtube	14,901	13,552,130	909.48
		Twitter	304,692	131,151,083	430.44
		Flickr	35,314	6,548,830	185.45
2018	GEM [28]	GEM-graph	8M	10M	1.67
	HERec [36]	Yelp	95,110	488,120	5.13
		Douban Book	138,423	1,026,046	7.41
		Douban Movie	90,241	1,714,941	19.00
	metapath2vec [9]	DBIS	78,366	326,481	4.17
		AMiner CS	12,522,027	14,215,558	1.14
	mvn2vec [37]	Twitter	116,408	183,341	1.57
		Youtube	14,900	7,977,881	535.43
		Snapchat	7,406,859	131,729,903	17.78
2019	GATNE [6]	Alibaba-S	6,163	17,865	2.90
		Amazon-GATNE	312,320	7,500,100	24.01
		YouTube	15,088	13,628,895	903.29
		Twitter	456,626	15,367,315	33.65
		Alibaba	41,991,048	571,892,183	13.62
	GTN [49]	DBLP	26128	239,566	9.17
	HAN [42]	IMDB	21420	86,642	4.04
		ACM	10942	547,872	50.07
	HeGAN [16]	Yelp	3,913	38,680	9.88
		DBLP	37,791	170,794	4.52
		Aminer	312,776	599,951	1.92
		Movielens	10,038	1,014,164	101.03
	HetGNN [50]	Academic II	49,708	137,286	2.76
		Academic I	272,272	544,976	2.00
		CDs Review	123,736	555,050	4.49
		Movie Review	74,701	629,125	8.42
2020	HGT [18]	ogbn-mag	179M	2B	11.17
	HNE [46]	PubMed	63,109	244,986	3.88
	MAGNN [13]	LastFM-r	71,689	3,034,763	42.33
	MV-ACM [52]	Amazon	10,099	113,637	11.25
		Alibaba	40,324	149,587	3.71
		Twitter	40,000	1,028,364	25.71
		PPI	15,005	1,044,541	69.61
		Youtube	2,000	1,114,025	557.01
		Aminer	178,385	5,935,349	33.27
2021	HGB [30]	LastFM	20,612	141,521	6.87
		Amazon	10,099	148,659	14.72
		Freebase	180,098	148,659	0.83
		Movielens	43,567	539,300	12.38
		Amazon-book	95,594	846,434	8.85
		Yelp-2018	91,457	1,183,610	12.94
	xFraud (ours)	eBay-small	288,853	612,904	2.12
		eBay-large	8,857,866	13,158,984	1.49
		eBay-xlarge	1.1B	3.7B	3.36

B DATASET CONSTRUCTION

In the transaction records, there exist a rich set of relations when two transactions share some linkage entities, e.g., executed by the same buyer, using the same payment instrument, shipped to the same address.

Following the same graph construction protocol, we construct *heterogeneous graphs* out of the transaction records in different scales — *eBay-xlarge*, *eBay-large*, and *eBay-small*. Note that *eBay-large* and *eBay-small* are subsets of *eBay-xlarge*. The graph construction protocol is as follows. Both transaction and linkage entities are treated as nodes. If an entity is used in a transaction, we create an edge between the transaction node and that entity (see Sec. 3.1). Only transaction node has input features.

Table 6: Node type counts $|\mathcal{V}_t|$ in heterogeneous graphs.

Dataset	Node type	#Count	Node type%
eBay-xlarge	txn	857M	77%
	pmt	81M	7%
	email	72M	6%
	addr	62M	5%
	buyer	69M	5%
eBay-large	txn	3,752,225	42.40%
	pmt	1,180,114	13.30%
	email	1,307,179	14.80%
	addr	1,316,251	14.90%
	buyer	1,302,097	14.60%
eBay-small	txn	207,749	71.90%
	pmt	22,273	7.70%
	email	25,878	9.00%
	addr	7,138	2.40%
	buyer	25,815	9.00%

We construct three datasets from the historical transactions at eBay. Historical transaction records were sampled to generate three datasets with different scales. Note that the ratio of fraudulent transactions is usually much smaller than that of the legitimate ones; hence, we try to down sample the benign transactions to alleviate the class imbalance problem.

eBay-xlarge. It is a billion-scale dataset of 1.1 billion nodes and 3.7 billion edges, which contains seven months of selected transaction records. The dimension of transaction features is 480.

eBay-large. All the historical transaction records spanning a given period in *eBay-xlarge* are sampled. The dimension of transaction features is 480. The linking entities whose transaction numbers below a predefined threshold are removed to maintain graph connectivity, which means that there is no isolated transaction in the graph.

eBay-small. We take a subset of *eBay-large* to construct *eBay-small* by shrinking the transaction spanning period, and the dimension of transaction features is 114.

For all three datasets, to further reduce the graph size while preserving graph connectivity, we adopt a graph sampling strategy: (1) All fraudulent transactions and randomly sampled benign transactions are selected as seeds. (2) Each seed is expanded to its k-hop neighbors, and at each hop, no more than N neighbors are picked. (3) The neighborhoods around the seeds with transaction numbers less than five are filtered out. We have a similar graph sampling across all datasets: for *eBay-xlarge*, $k = 8, N = 512$, for *eBay-large* and *eBay-small* $k = 3, N = 32$.

In addition, for the *eBay-xlarge* dataset, we produce the training/testing labels via two filtering and sampling steps:

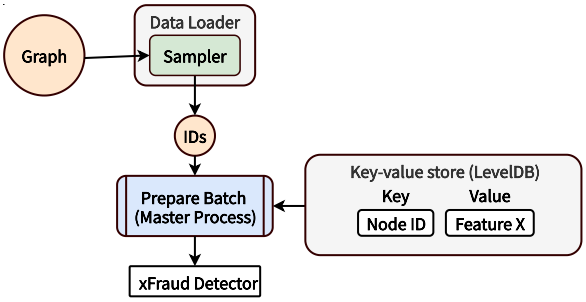

Figure 12: (Previous implementation) Using a single threaded KVStore to interact with GNN on a single machine.

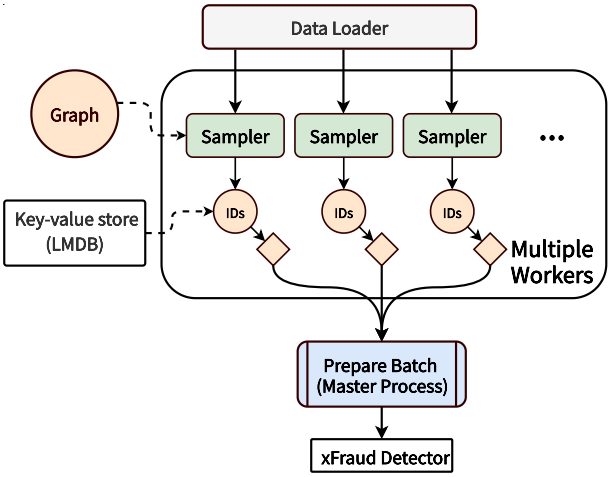

Figure 13: (New implementation) Using a multi threaded KVStore to interact with GNN on a single machine.

(1) The original data stream has a fraud rate = 0.016%.
(2) We then use some simple rules to filter out certain low-risk transactions. These rules are already implemented in the eBay transaction platforms to filter transactions. This is similar to what GEM [28] does in graph preprocessing and is also consistent with how this model will be used in practice. After this step, we have a fraud rate = 0.043%.
(3) To create the training and testing labels, we sampled all fraud transactions, and 1% of non-fraud transactions. Note that the other transactions are still in the graph, but without supervised labels. This gives us the *eBay-xlarge* dataset with a fraud rate = 4.33%.

The ratio of transaction frauds is 4.33%, 3.57%, and 4.30%, in *eBay-xlarge*, *eBay-large*, and *eBay-small*. respectively. We further summarize the distribution of each node type in Table 6.

C MORE DETAILS ON THE DISTRIBUTED XFRAUD DETECTOR

We introduce the experimental protocols and an extensive set of results on our billion-scale dataset *eBay-xlarge*.

Implementation of KVStores. We have implemented two types of KVStores when optimizing xFraud detector+. The multi threaded KVStore solution is used in the distributed setting. We show the detailed implementation of the interaction between GNN and the single threaded KVstore and the multi threaded KVStore in Figure 12 and 13, respectively. With this new optimization, we manage to reduce the training (incl. data loading) on the *eBay-large* to 1 minute per epoch. In comparison, a single-threaded KVStore on the same dataset would take 45 min/epoch.

Further experimental details for detector.

- *Machines.* We conduct the single-machine experiments on a Linux server with 16 Intel Xeon Gold 6230 CPU, one Nvidia Tesla V100 32 GB GPU, and 256 GB memory. For the distributed settings, we use a set of machines, each of which has 4 Intel Xeon Gold 6230 CPU, one Nvidia Tesla V100 32 GB GPU, and 32 GB memory.
- *Hyperparameters.* The baselines and xFraud detector+ are trained with this set of hyperparameters: *n_hid* = 400, *n_heads* = 8, *n_layers* = 6, *dropout* = 0.2, *optimizer* = *"adamw"*, *clip* = 0.25, *max_epochs* = 128, *patience* = 32. We keep the same set of hyperparameters for all datasets.

Further experimental results. We present the complete results in Table 7 on two different seeds (A and B) using 8 machines and 16 machines.

Convergence on eBay-xlarge. In this paragraph, we discuss the model convergence under different settings. In Figure 14, the models trained on 16 machines do not converge faster than that on 8 machines. Also, the final AUCs on 16 machines are worse compared to those on 8 machines. In this case, training using 8 machines is a better choice across different models using the current graph partitioning strategy as described in Sec. 4.

D EXPERIMENTAL DETAILS OF A MODIFIED GNNEXPLAINER

We implement GNNExplainer using the trained xFraud detector, transaction features, node index (of node-to-explain), edge indices, edge types, and node types as input. We obtain node feature masks of the subgraph as output, as well as the edge masks. The hyperparameters of GNNExplainer are: *epochs* = 100, $lr = 0.01$, $\beta_{\text{edge\_size}} = 0.005$, $\beta_{\text{node\_feature\_size}} = 1$, $\beta_{\text{edge\_entropy}} = 1$, $\beta_{\text{node\_feature\_size}} = 0.1$. The xFraud detector is not retrained during the explanation process.

We extend the vanilla GNNExplainer [47] so that it generates node feature masks for all the nodes, which enables a node-level feature explanation to a prediction. Learning the feature importance of all node features was not possible with the vanilla GNNExplainer. The training of explainer is initialized with a random edge mask $1 \times |\mathcal{E}|$ and a random node feature mask $|\mathcal{V}| \times F$ (F the size of node features), as well as four random coefficients of edge size β_{es}, node feature size β_{nfs}, edge entropy β_{ee}, and node feature entropy β_{nfe}. It then takes the node index of node-to-explain, transaction features, node types, edge types and edge indices as input. The explainer takes the weights trained in the detector and uses only the detector model in the evaluation mode, as Figure 4 demonstrates (right). The loss function of explainer has to include edge entropy and node feature entropy so that the explainer knows which important nodes,

Table 7: Model performance in distributed settings on *eBay-xlarge* (# epochs: 128). The best score of a column is in bold.

Model	# of machines	Seed	Accuracy	AP	AUC	Training time (s/epoch)	Inference time (s/batch)
GAT	8	A	0.9334	0.4478	0.8894	62.62	0.0557 ± 0.1966
		B	0.9309	0.4120	0.8863	62.85	
	16	A	0.9348	0.4481	0.8894	**32.08**	
		B	0.9425	0.3932	0.8838	34.14	
GEM	8	A	0.9554	0.4513	0.8960	61.67	**0.0167± 0.0054**
		B	0.9578	0.4613	0.8962	61.86	
	16	A	0.9552	0.4349	0.8949	33.40	
		B	0.9574	0.4363	0.8926	33.71	
xFraud detector+	8	A	0.9701	**0.5942**	**0.9074**	71.79	0.0799 ± 0.1868
		B	**0.9703**	0.5931	0.9073	69.15	
	16	A	0.9694	0.5483	0.8900	37.35	
		B	0.9650	0.4932	0.8883	40.09	

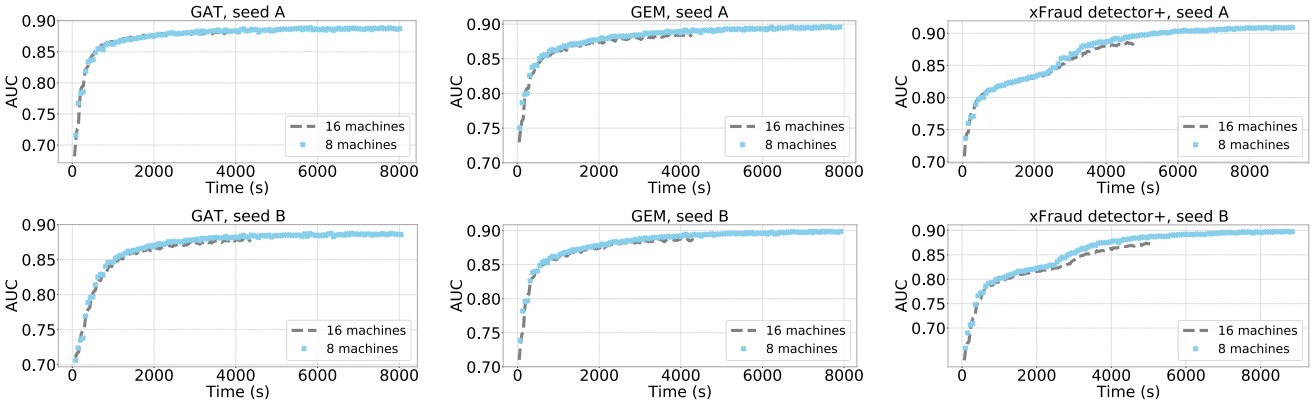

Figure 14: Convergence of distributed training (8 vs. 16 machines) on GAT, GEM, and xFraud detector+, measured by AUC (on two seeds).

node features and edges to attend in predicting the current node. The goal of explainer loss is to jointly minimize the detector loss with the entropy of node features and edges.

To compute the explainer loss, we first compute the edge mask and node feature mask of the subgraph S in G that contributes to the node-to-explain. We use M_{E_S} to denote the edge mask in the subgraph S (S a subgraph of G), and we have $M_{E_S} = \sigma(E_S)$, E_S a random initialization of edge parameters. Likewise, we denote the node feature mask as $M_{V_S} = \sigma(V_S)$, V_S a random initialization of node feature parameters. Now we calculate the explainer loss in three parts, detector loss (eq. 1), edge entropy (eq. 2), and node feature entropy (eq. 3). We finally sum them up to form the explainer loss:

$$\sum_i C_i \log(S_i), \tag{1}$$

$$\beta_{\text{es}} \sum M_{E_S} + \beta_{\text{ee}} \frac{\sum \Big(- M_{E_S} \log(M_{E_S} + \epsilon) - (1 - M_{E_S}) \log(1 - M_{E_S} + \epsilon) \Big)}{|\mathcal{V}_{\mathcal{E}}|}, \tag{2}$$

$$\beta_{\text{nfs}} \frac{\sum M_{V_S}}{|\mathcal{V}_{\mathcal{S}}|} + \beta_{\text{nfe}} \frac{\sum \Big(- M_{V_S} \log(M_{V_S} + \epsilon) - (1 - M_{V_S}) \log(1 - M_{V_S} + \epsilon) \Big)}{|\mathcal{V}_{\mathcal{S}}|}, \tag{3}$$

where $i \in \{\text{labeled transactions}\}$, C_i is the true label of a transaction, S_i the output of the *softmax* layer in DNN, $|\mathcal{V}_{\mathcal{S}}|$ and $|\mathcal{E}_{\mathcal{S}}|$ the number of nodes and edges in the subgraph S, and ϵ a small constant to prevent $\log(0)$. By back propagation, the new loss is used to compute the new network weights in explainer and thus the network has the capacity to learn the subgraph nodes and their features that most importantly contribute to certain predictions made by the detector.

E ANNOTATION, NODE IMPORTANCE, RANDOM VS. GNNEXPLAINER

Annotation protocol. Now we introduce our annotation protocol of human ground truth. The goal of annotation is to assign a node importance score to each node in terms of how important the node is when the seed node prediction is made. We do not perform

Table 8: Top$k$ hit rate between explainer edge weights and human annotations: GNNExplainer vs. random.

Top$k$ hit rate	Top5	Top10	Top15	Top20	Top25
Random	0.13	0.45	0.60	0.70	0.79
GNNExplainer	0.45	0.69	0.82	0.90	0.92
$\Delta(GNNExplainer - Random)$	0.32	0.24	0.22	0.20	0.13

annotations on the edge level because the annotators only have access to node-level information (e.g., node features and representations). We have five expert annotators to ensure that each node is at least annotated by two annotators. There are three scales of node importance the annotators can assign: 0, 1, 2 for low, medium, and high importance, respectively. Then, we calculate the average inter-annotator agreement (IAA) score of annotator pairs. The average IAA score is 0.532 among 10 pairs of annotators, with the highest IAA 0.773 and lowest 0.314. But how do we know if our annotations are of high quality? Assuming the human annotators were randomly assigning scores, we employ random integer generators that assign 0, 1, 2 to replace all the annotations by human, and we calculate the average IAA score among the random annotators. Also, we repeat this random experiment 10 times and calculate the mean IAA score. The random IAA score is -0.006 which is significantly worse compared with 0.525, the IAA score of human annotators.

Node importance score. After we have obtained the human annotations by five annotators, we first calculate the average node importance score for a node v by $\frac{\sum annotation_i}{5}$, where an annotator $i \in [1, 2, 3, 4, 5]$. We then use these node importance scores to compute the edge importance scores. There are three strategies to calculate the edge importance based on its incident nodes — by averaging ("avg") or summing ("sum") the node importance scores, or by taking the minimal node importance score ("min"). There is no theoretical or empirical evidence of which aggregation method is the best, we therefore have run all the aggregation methods and select the one that performs the best.

Topk hit rate. In Figure 6, we demonstrate two graphs with edge importance scores and edge weights, respectively. We have to choose a meaningful set of k. Note that the average count of total edges across the communities is 81.56, among which the average count of edges with the largest edge importance is 20.90. This means that as long as k is smaller than or around 20, the top$k$ hit rate reflects a meaningful agreement score between the explainer and the annotators in ranking the important edges.

Random vs. GNNExplainer. Another caveat of the top$k$ edge selection is that we need to break the tie among the largest edge importance scores. To tackle this, we randomly draw 100 samples when selecting the top$k$ edges based on the highest importance score. Then, we take the average hit rate of these 100 draws. We have also run experiments with 10,000 draws, which renders similar results reported in Table 8. Here, we report the hit rates computed as the mean of random 100 draws.

In Table 8 we report the top$k$ hit rate with $k \in [5, 10, 15, 20, 25]$. Our hit rate is already 45% when inspecting the top 5 edges and increases as k increases. To draw the conclusion that the explainer agrees strongly with our human annotators, we look at a random baseline. The random baseline assumes that the explainer randomly assigns edge weights during prediction. We let a random number generator assign edge weights to each edge and we compute the top$k$ hit rate between random edge weights and edge importance scores. We repeat the random experiment 10 times, and finally obtain the average top$k$ hit rate from these 10 random draws. The random baseline is also reported in Table 8. Taking the difference between our hit rate and the random one, we see the largest discrepancy is at the top 5 hit rate and gradually drops as k increases. This demonstrates the strong agreement between the actual explainer weights and our human annotators.[7]

Comparing aggregation methods in analyzing explainer weights. There are three different aggregation strategies, ranging from node importance (human) to edge importance (human). In Tables 9, 10 and 11, there is no substantial difference in results generated by averaging, summing, or minimizing the weights. Also, in communities with a benign (0)/fraudulent (1) node-to-predict, there is no substantial difference. We also ran a paired-t-test to see if the distributions between these two types of communities are identical: the test results do not allow us to reject this null hypothesis on a significance level of 0.05. Therefore, in the follow-up experiments of hybrid explainer, we always use "averaging" as the aggregation method to compute the edge importance score (human).

Table 9: Top$k$ hit rate between explainer edge weights ("avg") and human annotations: GNNExplainer vs. random. $c1$: a community labeled 1, $c0$: a community labeled 0.

Top$k$ hit rate	Top5	Top10	Top15	Top20	Top25
Random	0.13	0.45	0.60	0.70	0.79
GNNExplainer	0.45	0.69	0.82	0.90	0.92
$\Delta(GNNExplainer - Random)$	0.32	0.24	0.22	0.20	0.13
$Random_{c0}$	0.31	0.20	0.21	0.20	0.15
$GNNExplainer_{c0}$	0.47	0.77	0.90	0.97	1.00
Δ_{c0}(GNNExplainer-Random)	0.16	0.57	0.69	0.27	0.85
$Random_{c1}$	0.33	0.17	0.23	0.21	0.11
$GNNExplainer_{c1}$	0.41	0.59	0.72	0.81	0.82
Δ_{c1}(GNNExplainer-Random)	0.08	0.42	0.49	0.60	0.71

F MORE DETAILS ON THE HYBRID EXPLAINER

Centrality measures as edge weights. We use the following two ways to compute edge weights using centrality measures:

(1) Compute the edge weights based on the node annotations using edge centrality measures such as **edge betweenness** and **edge load centrality**. Edge betweenness measures the number of the shortest paths between vertices that contain the edge, normalized by $\frac{2}{n(n-1)}$ in an undirected graph. Edge load counts the number of

[7] Comparing results from three aggregation methods ("sum" vs. "min" vs. "avg"), there is no significant difference in the distribution of our hit rates and $\Delta(GNNExplainer - Random)$. We hence report only the results of "avg". In addition, there is no substantial difference between $\Delta(GNNExplainer - Random)$ of communities labeled 1 and 0. For more details of the results on "min" and "sum" and their performances on communities labeled 1 and 0.

Table 10: Top$k$ hit rate between explainer edge weights ("min") and human annotations: GNNExplainer vs. random. $c1$: a community labeled 1, $c0$: a community labeled 0.

Top$k$ hit rate	Top5	Top10	Top15	Top20	Top25
Random	0.13	0.45	0.60	0.70	0.79
GNNExplainer	0.45	0.69	0.82	0.90	0.92
$\Delta(GNNExplainer - Random)$	0.32	0.24	0.22	0.20	0.13
$Random_{c0}$	0.16	0.48	0.69	0.77	0.85
$GNNExplainer_{c0}$	0.47	0.77	0.90	0.97	1.00
Δ_{c0}(GNNExplainer-Random)	0.31	0.29	0.21	0.20	0.15
$Random_{c1}$	0.08	0.42	0.49	0.60	0.71
$GNNExplainer_{c1}$	0.41	0.59	0.72	0.81	0.82
Δ_{c1}(GNNExplainer-Random)	0.33	0.17	0.23	0.21	0.11

Table 11: Top$k$ hit rate between explainer edge weights ("sum") and human annotations: GNNExplainer vs. random. $c1$: a community labeled 1, $c0$: a community labeled 0.

Top$k$ hit rate	Top5	Top10	Top15	Top20	Top25
Random	0.10	0.38	0.54	0.63	0.77
GNNExplainer	0.38	0.63	0.80	0.88	0.90
$\Delta(GNNExplainer - Random)$	0.28	0.25	0.26	0.25	0.13
$Random_{c0}$	0.17	0.40	0.61	0.70	0.85
$GNNExplainer_{c0}$	0.41	0.70	0.90	0.97	1.00
Δ_{c0}(GNNExplainer-Random)	0.24	0.30	0.29	0.27	0.15
$Random_{c1}$	0.03	0.37	0.45	0.56	0.67
$GNNExplainer_{c1}$	0.36	0.55	0.68	0.77	0.78
Δ_{c1}(GNNExplainer-Random)	0.33	0.18	0.23	0.21	0.11

the shortest paths which cross each edge. Then, we calculate the top$k$ hit rate between the edge centrality scores and the human annotations.

(2) Compute the edge weights based on the node annotations after transforming the original graph into a line graph. We compute various types of **node centralities** (e.g., closeness, eigenvector centrality, degree, etc.) measures in the line graph.

We report the results of representing edge weights with 13 centrality measures in Table 1. We compute the centrality measures using the *networkx*[8] package in Python.

Observations on comparing explainer weights and centrality measures. We observe that the hit rates computed by explainer weights $H(e)$ and by different centrality measures $H(c)$ are close. The similar hit rates show that GNNExplainer and centrality measures both manage to learn the most important edges when filtering the fraudulent transactions. For each rank, we mark the highest hit rate with bold: there is not a centrality measure that consistently outperforms the remaining measures. Even among various centrality measures, the $\Delta(H(e) - H(c))$ on different ranks vary. As k increases, the differences between the hit rates decrease.

We pick the best four centrality measures according to the hit rate, i.e., edge betweenness, degree, edge load, closeness and harmonic. If we examine the differences of hit rate $\Delta(H(e) - H(c))$ across communities in Figure 7, we notice that there is no clear winner between $H(e)$ and $H(c)$ in detecting the most important edges when comparing to human annotations. More importantly, a trade-off between $H(e)$ and $H(c)$ can be observed. This motivates us to learn a hybrid explainer using both explainer weights and centrality measures.

A hybrid learner that incorporates both explainer weights and centrality measures. We formulate the learning problem as follows. First, we learn two coefficients — centrality coefficient A and explainer coefficient B, which maximizes $avg(H(h))$ in the training communities via $avg(A * w(c) + B * w(e))$, where $w(c)$ denotes the centrality measures, and $w(e)$ the explainer weights. Since there are 41 communities, we take the first 21 communities as the training set and the last 20 as the test set. Then, we calculate $avg(H(h))$ in the test communities using the A and B learned over the training set. There are various techniques to optimize $avg(A * w(c)+B*w(e))$ and search for the optimal A and B, which maximize the average $H(h)$ in the training set. By taking a centrality measure that generates the best $H(c)_{Top5}$ in Table 1 (edge betweenness), we have run these three sets of experiments to optimize A and B:

(1) Fit polynomial functions where we find the best feature degree to maximize the average $H(h)$ in the training communities;
(2) Grid searches for A, where $B = 1 - A$;
(3) Train Ridge linear regressions on $avg(A * w(c) + B * w(e))$, where we also optimize the regularization hyperparameter α.

We run (1) to find the best degree d among {1, 2, ..., 9} and obtain $d = 1$ being the best fit, i.e., a linear combination of $A*w(c)+B*w(e)$. We illustrate the results of hybrid explainers constructed by (2) and (3) in Table 12. For the grid search in (2), we tune A in {0.00, 0.01, ..., 1.00}, where A maximizes the average hit rate in the training communities. For (3), the best α is 0.99 among {0.01, 0.02, ..., 0.99}, with $A = -0.1097, B = 0.1064$. If we compare the results of $H(h)$, $H(c)$, and $H(e)$ at all ranks, the hybrid learner has achieved at least a result as good as $H(c)$ if not better.

The results in Table 1 and Figure 7 validate that our proposed hybrid explainer can achieve a trade-off between the centrality measures and explainer weights. Both measures agree with human annotators, and we can leverage weights learned by explainer and centrality to construct a better explainer. This hybrid explainer incorporates both the topological features of the community and the message passing learned via GNNExplainer.

Moreover, we have also noticed that the centrality measures assign identical weights to many edges in the community. In contrast, the vanilla GNNExplainer always assigns a total order of weights to the edges, with the edges closer to the node-to-explain getting the highest weights. GNNExplainer offers a local explanation of the prediction, while centrality measures attend to the global structure of the community. Intuitively, by combining the best of both worlds, the hybrid explainer is beneficial since it considers both local and global structures of communities.

More Results on the Hybrid Explainer. We report the hit rate of top 5 edges across GNNExplainer, edge betweenness centrality, and the hybrid explainer trained using Ridge and grid search in Table 12.

[8] https://networkx.org/documentation/stable/reference/algorithms/centrality.html (last accessed: Sep 1, 2021).

Table 12: Top$k$ hit rate in the train and test communities by the hybrid explainer. A is the coefficient of centrality weights (edge betweenness) in the hybrid explainer $A*w(c)+B*w(e)$, where $B=1-A$.

H(_)	Edge betweenness $H(c)$		GNNExplainer $H(e)$		Hybrid (ridge) $H(h)$		Hybrid (grid) $H(h)$		
	Train	Test	Train	Test	Train	Test	Train	Test	A_{Train}
Top5	0.4817	0.45540	0.44257	0.44800	0.44648	0.44890	0.45971	**0.45550**	0.75
Top10	0.6581	0.78175	0.61210	0.77580	0.60767	**0.81115**	0.61881	0.78700	0.94
Top15	0.7497	0.87763	0.75981	0.88473	0.74838	0.89210	0.76375	**0.89410**	0.91
Top20	0.8459	0.96205	0.84126	0.95840	0.83505	0.96198	0.85595	**0.96275**	1.00
Top25	0.8813	**0.96616**	0.88350	0.95954	0.88286	0.96614	0.88379	0.96614	0.64
Top30	0.8868	0.96705	0.88778	0.95893	0.88790	**0.96780**	0.88938	**0.96780**	0.65
Top35	0.8920	**0.95780**	0.89388	0.94731	0.89339	0.95761	0.89444	0.95771	0.51
Top40	0.8976	0.93659	0.89860	0.92608	0.89893	0.93673	0.89917	**0.93764**	0.68
Top45	0.9026	0.91598	0.90244	0.90678	0.90443	**0.91608**	0.90472	0.91607	0.68

G CASE STUDIES USING HYBRID EXPLAINER

In this paper, a fraudulent transaction is marked as 1 (positive) and a benign one as 0. When we report true positives (TP), true negatives (TN), false positives (FP), and false negatives (FN), these four cases correspond to the following detection scenarios: "TP" – fraudulent transactions being flagged correctly, "TN" – benign transactions being flagged correctly, "FN" – we have missed frauds in detection, "FP" – benign transactions wrongly flagged as fraud.

G.1 More true positive cases

Except the case we show in Figure 16, we present six more TP cases in our 41 communities, visualized using weights learned in the hybrid explainer. We see from the visualization in (a), (c), and (f), xFraud does a good job in detecting suspicious transaction, even if the frequencies of fraudulent/benign cases are close. xFraud hybrid explainer not only manages to learn from the incident edges of the node-to-predicts, but also learns the path where the risk propagates. For instance, in (b), it learns that transaction 0 connects linking entities 17 (payment token) and 18 (email) with node 37 (buyer), which influences strongly the prediction of node 36 to be fraud. This type of risk propagation is useful in learning the embedding representations of linking entities. Similar to (b), we also observe a clear risk propagation path in (e). In case (d), we observe a typical fraudulent cluster which could be due to the fact that a valid payment token (node 19) was used at the beginning to gain the trust of the platform, then the defaulter conducts many fraudulent transactions. It could also be that the defaulter has hacked one payment token (node 5) and uses that payment token to conduct many transactions in a short time. In either case, the xFraud can assist BU to identify this kind of fraud cluster.

G.2 More case studies: false positives and false negatives

We investigate several case studies for the conditions "FP" and "FN" and share our insights.

False positive (FP): benign → fraud. In the community illustrated in Figure 17 (a), we have one buyer/email address/payment token and two shipping addresses. One shipping address (node 6) is much more frequently used than the other one. Note that this heavily used shipping address (node 6) is linked to many fraudulent transactions. This makes the prediction of seed node 39 prone to fraudulent (probability = 0.972 in xFraud detector+), because this transaction is directly linked to seed 6, which is considered highly suspicious by learning from its neighbors in the community. The most important edges in generating the prediction are marked in bold (0-6, 0-8). However, BU reports that this account is not fraudulent after investigation. Similarly, we have more fraudulent cases in the communities than the benign ones in the cases shown in Figure 17 (b) and 17 (c).

False negative (FN): fraud → benign. In a community like Figures 17 (d), where multiple buyers/payment tokens/email/shipping addresses are involved, we do not observe that one shipping address is used more frequently in the transaction logs. However, there are much more benign cases in the neighborhood, therefore xFraud detector+ has problems identifying a fraudulent transaction which could be due to a sudden attack, or a delay of user chargebacks. In Figure 17 (f) we see a simple (single-buyer) community with more fraudulent transactions than benign ones in the neighborhood. However, since the important (thick) edges are connected to more benign transactions than frauds (benign: 2, 14, 8, 9, 13, 11; fraud: 21, 17, 0), the node 1 is classified wrongly as benign.

To empirically investigate the case studies, we show in Table 13 that the different conditions are indeed correlated with communities types. We do not have false positives (benign wrongly recognized as fraudulent) in the complex communities, and xFraud does a better job in communities with more than one buyer.

To summarize the **FP: benign → fraud** cases, in all the FP cases we have (6 out of 6), there is only one buyer in the community, one linking entity of each type (i.e., one email, one payment token, one shipping address). Even if there are two linking entities, one is always more frequently used than the other one, and the seed is linked to the entity that is more frequently used. Whenever there is more fraudulent transactions connected to that linking entity, the benign node-to-predict is classified as fraudulent; vice versa for false negatives (2 out of 8). This is preemptive in risk prevention; the user might expect some short-term interruption of the service while being alert and notified by the platform that a fraudulent transaction might be ongoing.

In summary, the **FN: fraud → benign** cases show more variability, and our goal is to avoid as much as possible the false negatives. In many of the cases (6 out of 8), we see more buyers and linking entities (such as payment tokens and emails) in the community – we have higher false negatives in the complex communities. It is hard for xFraud detector+ to distinguish signals sent via various buyers and transactions. It could be deliberate ring attacks with accounts "cultivated" over a long time, or could be a one-time attack of one account using an unknown device.

G.3 System limitation and possible causes.

As we see in most of the cases, the misclassification of frauds is related to the ratio of fraudulent/benign cases in the k-hop neighborhood of the node-to-predict. It is therefore important to enforce a graph partition constraint of benign/fraudulent-ratio, so that the prediction is not strongly influenced by the frequency of cases. This goes into the direction we discussed before in the scalability experiments of *eBay-xlarge*: how to scale out training in a distributed setting on a heterogeneous graph.

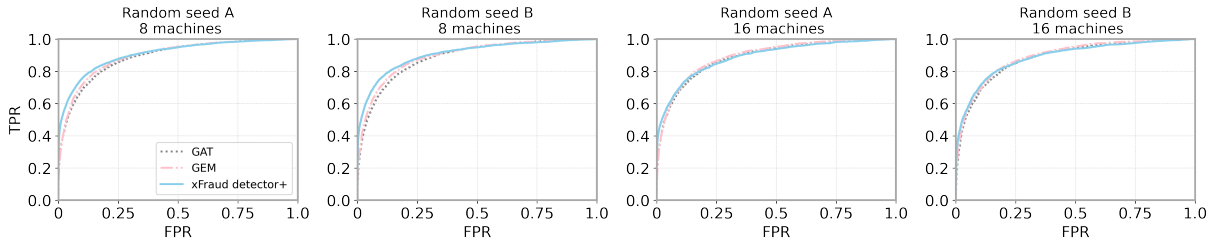

Figure 15: ROC curves using different settings (seeds and # machines) on *eBay-xlarge*.

Table 13: Confusion matrix of TP, TN, FP, and FN in simple and complex communities. The sample is the 41 communities we present in Sec. 5.1. We show the frequency and percentage of one condition in one type of communities in the bracket, where a simple community has only one buyer, and a complex one has more than one buyer. "TP": fraudulent transactions, "TN": benign transactions, "FN": missed frauds in detection, "FP": benign flagged as fraud.

Simple communities (16, 100%)		Complex communities (25, 100%)	
FP (6, 37.5%)	**TP** (4, 25%)	**FP** (0, 0%)	**TP** (6, 24%)
FN (2, 12.5%)	**TN** (4, 25%)	**FN** (6, 24%)	**TN** (13, 52%)

Although our system can flag some guest checkouts that are linked to suspicious entities, it still remains a difficult use case to capture with both ML and GNN methods. Guest checkout allows users to make purchases without logging and to stay anonymous. Our xFraud detector is designed for graph, therefore it requires purchases linked to some existing and nontrivial entities. Image a case where the user chooses a guest checkout to make a purchase. The email is newly registered, so it is not linked to any existing entities. The ip address is from a public places such as cafe or gas station. The payment token is a credit card which have not been used in our checkout system. The shipping address is a public transshipment warehouse. In such a case, none of the trivial entities can be linked by this purchase, so that our xFraud detector can hardly retrieve any useful information to make accurate predictions on the purchase.

H MORE EVALUATION METRICS OF EXPERIMENTS ON EBAY-LARGE

H.1 True positive rate (TPR)/Recall, true negative rate (TNR), false positive rate (FPR), false negative rate (FNR)

We document the TPR, TNR, FPR, and FNR on the test set of *eBay-xlarge* in Tables 14, 15, and 16. Note that FPR = 1 - TNR and FNR = 1 - TPR. TPR is also known as recall.

H.2 Precision and recall at various thresholds

In Tables 17, 18, and 19, we list the precision and recall scores calculated at various thresholds on the test set of *eBay-xlarge*.

H.3 *ROC curve on eBay-large.*

Besides the ROC curve in Figure 9 showing FPR <0.1 in flagging frauds on *eBay-large*, we also present the ROC curves in the full range of FPR. The xFraud detector+ outperforms all baselines in ROC-AUC in the two experiments on 8 and 16 machines, respectively.

H.4 Discussion: Performance analysis of xFraud in production

Reading from Tables 18 and 19, on the whole test set of *eBay-xlarge* with 4.33% fraud rate, our method

- with threshold 0.983 has precision = 0.9822 and recall = 0.1091,
- with threshold 0.977 has precision = 0.9539 and recall = 0.2063,
- with threshold 0.960 has precision = 0.9217 and recall = 0.2930.

As we discussed in Appendix B, we filtered and sampled the transaction labels in the *eBay-xlarge* dataset before applying GNN models. These operations lead to the change of fraud rate in the transaction labels in each step:

(1) the original data stream (0.016% fraud)
[filtered by rules] ⇓
(2) the filtered data stream (0.043% fraud)
[sampled all frauds & 1% benign] ⇓
(3) the sampled data stream (4.33% fraud) .

In this paper, we report all numbers on step (3). *How would the algorithm perform on the dataset on step (2)?* We further report precision on step (2). In this case, a 0.98 precision on (3) corresponds to 0.32 precision on (2), with 0.1 recall; and a 0.95 precision on (3) corresponds to 0.16 precision on (2), with 0.2 recall.

A 0.32 precision means that for 3 fraud candidates investigated by the business unit, 1 will be a real fraud. This, with 0.1 recall is acceptable in our scenario. Even a 0.16 precision, with 0.2 recall, is reasonable – for every 6 fraud candidates investigated by the business unit, 1 will be a real fraud.

When our model is deployed into production, there will be more considerations beyond this single GNN model — one has to consider the entire pipeline, including data preprocessing, feature engineering, and downsampling. For example, in many eBay applications, less risky transactions are filtered out by rule-based or ML-based strategies before using more complicated models such as GNN; and GEM [28] has also pre-filtered isolated transactions.

H.5 Potential production scenario using xFraud

We have used an industrial-scale dataset *eBay-xlarge* using seven months of transaction data produced at eBay. xFraud now has a model trained on historical data. What is also practical is an incremental setting of online model training and fine-tuning. For example, we can perform model updates on a daily basis to ensure the model timeliness. We can also build models in an incremental setting. For instance, we use the data from the $T-1$ week (or month) to flag the transactions produced in the T week (or month). However, there is a caveat here: many fraudulent behaviors are planned for the long-term attacks. The defaulters would "cultivate" a set of accounts for many months to gain the trust of the platform and then launch attacks. Hence, it is crucial to use both historical and up-to-date data to train our system and combine their predictions in production. After our delicate optimization for the distributed xFraud system, xFraud now can efficiently train a GNN model on a billion-scale graph dataset (38s per epoch on *eBay-xlarge* using 16 machines). With xFraud's powerful processing capabilities, we can train a new model within several hours in eBay, and hence support real production scenarios. Besides, xFraud can also accelerate the inference task significantly in a distributed setting (less than 0.1 seconds to process a batch of 640 nodes using a single machine). To help downstream tasks in a production scenario, the inference scores for the transactions are attached to the corresponding entities, represented as risk scores for the upcoming transaction events. These scores are treated as features for downstream risk models and as variables for the rule-based defense systems.

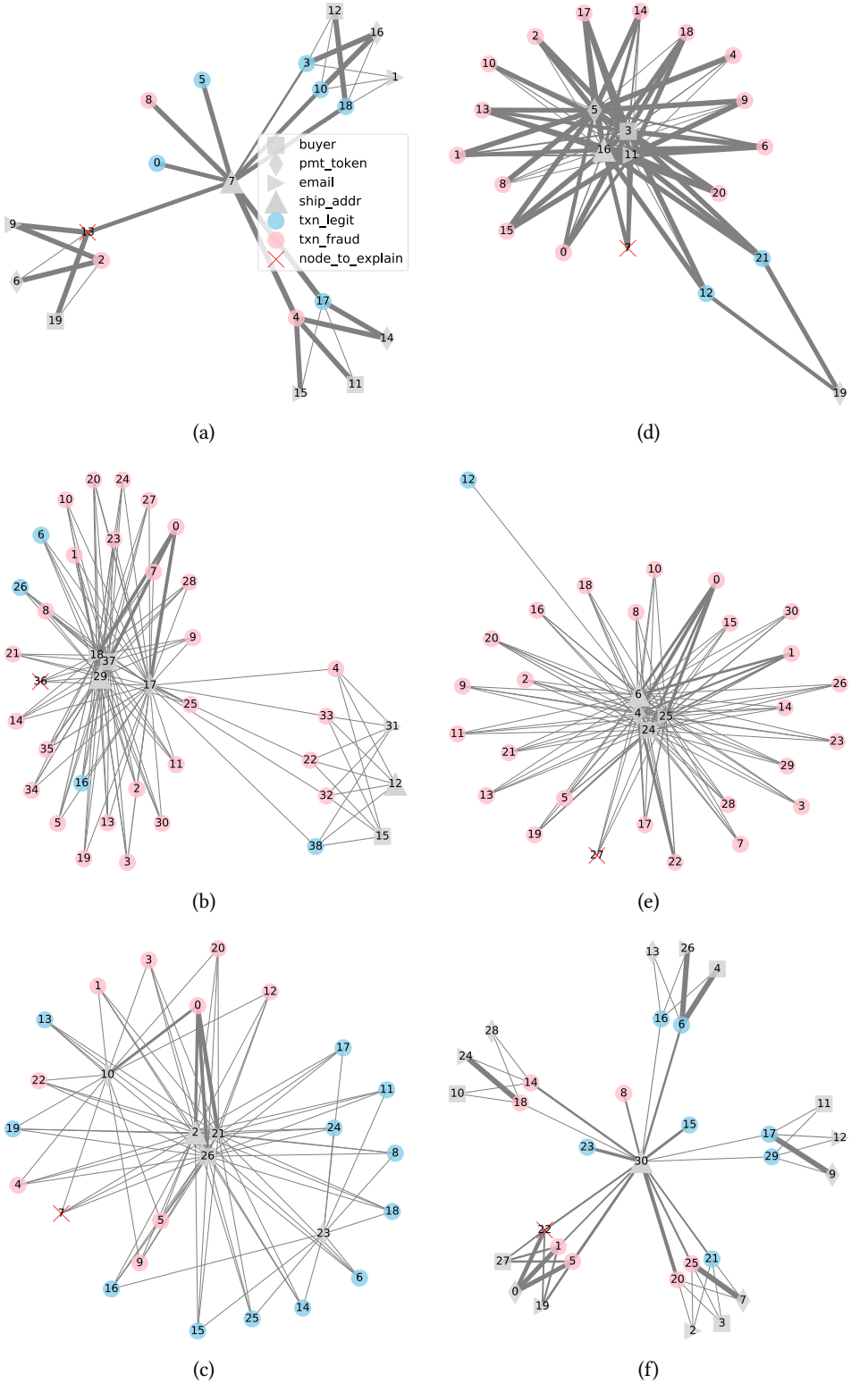

Figure 16: Case studies using hybrid learner weights: true positives (TP).

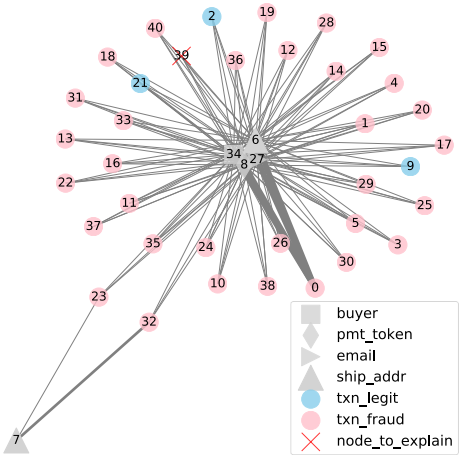

(a) FP: benign → fraudulent (case 1)

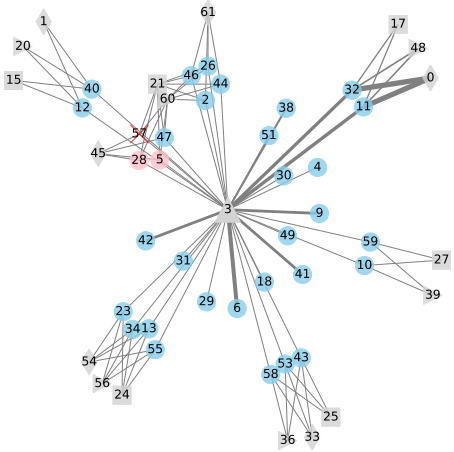

(d) FN: fraudulent → benign (case 1)

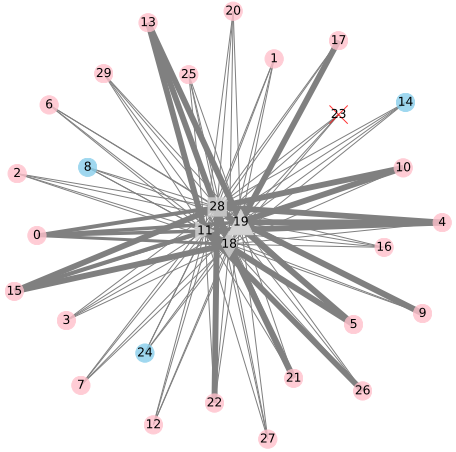

(b) FP: benign → fraudulent (case 2)

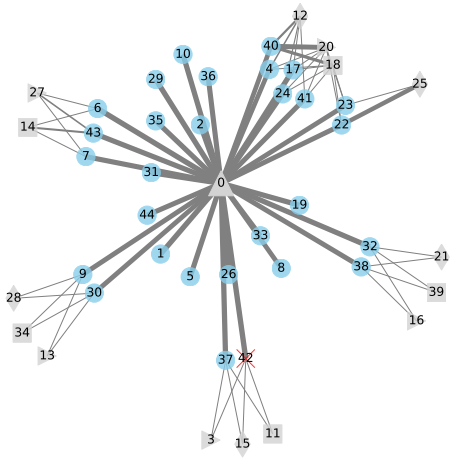

(e) FN: fraudulent → benign (case 2)

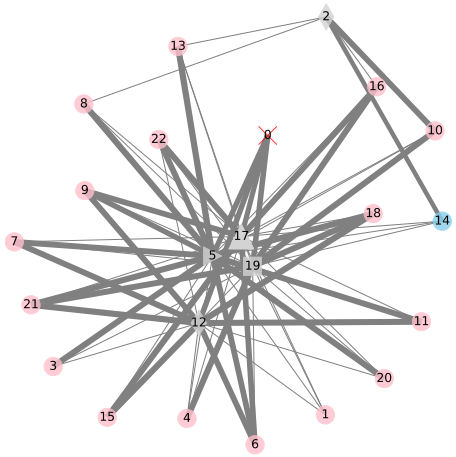

(c) FP: benign → fraudulent (case 3)

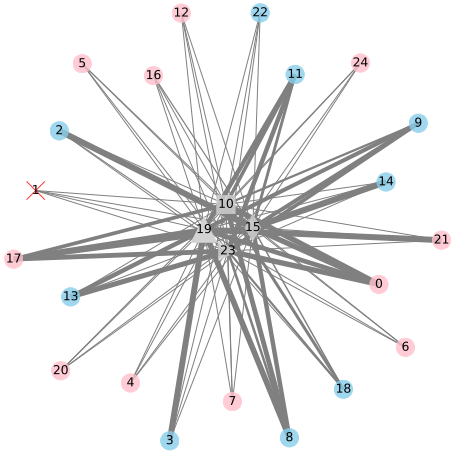

(f) FN: fraudulent → benign (case 3)

Figure 17: Case studies using hybrid learner weights: false positives (a,b,c on the left) and false negatives (d,e,f on the right).

Table 14: TPR, FNR, FPR, and TNR on *eBay-xlarge* by varying thresholds from 0.1 to 0.9 on the prediction scores. FNR = 1 - TPR. The higher TPR is, the better; the lower FNR, the better. FPR = 1 - TNR. The higher TNR is, the better; the lower FPR, the better.

Model	# of machines	Seed	TPR@threshold								
			0.1	0.2	0.3	0.4	0.5	0.6	0.7	0.8	0.9
GAT	8	A	0.7379	0.6718	0.6264	0.5891	0.5535	0.5158	0.4730	0.4187	0.3170
		B	0.7443	0.6664	0.6184	0.5787	0.5391	0.5030	0.4577	0.3972	0.2780
	16	A	0.7439	0.6789	0.6311	0.5923	0.5483	0.5112	0.4614	0.3790	0.2152
		B	0.7137	0.6287	0.5839	0.5396	0.4930	0.4345	0.3488	0.2262	0.0432
GEM	8	A	0.7125	0.6028	0.5182	0.4608	0.4058	0.3563	0.3086	0.2501	0.1599
		B	0.6737	0.5611	0.4913	0.4363	0.3788	0.3349	0.2902	0.2344	0.1360
	16	A	0.7052	0.6061	0.5263	0.4592	0.4073	0.3490	0.2859	0.2014	0.0660
		B	0.6649	0.5646	0.4955	0.4331	0.3829	0.3282	0.2522	0.1742	0.0588
xFraud detector+	8	A	0.5731	0.5083	0.4794	0.4582	0.4407	0.4268	0.4103	0.3933	0.3621
		B	0.5480	0.4801	0.4482	0.4213	0.4067	0.3904	0.3746	0.3579	0.3199
	16	A	0.5056	0.4521	0.4198	0.3978	0.3757	0.3526	0.3228	0.2794	0.1424
		B	0.5212	0.4549	0.4177	0.3902	0.3524	0.3113	0.2529	0.1597	0.0018

Model	# of machines	Seed	FNR@threshold								
			0.1	0.2	0.3	0.4	0.5	0.6	0.7	0.8	0.9
GAT	8	A	0.2621	0.3282	0.3736	0.4109	0.4465	0.4842	0.5270	0.5813	0.6830
		B	0.2557	0.3336	0.3816	0.4213	0.4609	0.4970	0.5423	0.6028	0.7220
	16	A	0.2561	0.3211	0.3689	0.4077	0.4517	0.4888	0.5386	0.6210	0.7848
		B	0.2863	0.3713	0.4161	0.4604	0.5070	0.5655	0.6512	0.7738	0.9568
GEM	8	A	0.2875	0.3972	0.4818	0.5392	0.5942	0.6437	0.6914	0.7499	0.8401
		B	0.3263	0.4389	0.5087	0.5637	0.6212	0.6651	0.7098	0.7656	0.8640
	16	A	0.2948	0.3939	0.4737	0.5408	0.5927	0.6510	0.7141	0.7986	0.9340
		B	0.3351	0.4354	0.5045	0.5669	0.6171	0.6718	0.7478	0.8258	0.9412
xFraud detector+	8	A	0.4269	0.4917	0.5206	0.5418	0.5593	0.5732	0.5897	0.6067	0.6379
		B	0.4520	0.5199	0.5518	0.5787	0.5933	0.6096	0.6254	0.6421	0.6801
	16	A	0.4944	0.5479	0.5802	0.6022	0.6243	0.6474	0.6772	0.7206	0.8576
		B	0.4788	0.5451	0.5823	0.6098	0.6476	0.6887	0.7471	0.8403	0.9982

Model	# of machines	Seed	TNR@threshold								
			0.1	0.2	0.3	0.4	0.5	0.6	0.7	0.8	0.9
GAT	8	A	0.8673	0.9077	0.9268	0.9400	0.9506	0.9597	0.9688	0.9777	0.9905
		B	0.8604	0.9041	0.9246	0.9380	0.9486	0.9586	0.9678	0.9779	0.9907
	16	A	0.8650	0.9057	0.9265	0.9403	0.9523	0.9631	0.9734	0.9837	0.9961
		B	0.8792	0.9166	0.9358	0.9501	0.9628	0.9730	0.9829	0.9933	0.9995
GEM	8	A	0.9019	0.9440	0.9621	0.9729	0.9802	0.9859	0.9903	0.9945	0.9981
		B	0.9189	0.9539	0.9697	0.9787	0.9840	0.9882	0.9924	0.9959	0.9989
	16	A	0.8987	0.9411	0.9600	0.9716	0.9799	0.9870	0.9918	0.9963	0.9995
		B	0.9134	0.9497	0.9662	0.9759	0.9834	0.9890	0.9934	0.9973	0.9997
xFraud detector+	8	A	0.9721	0.9856	0.9902	0.9927	0.9941	0.9952	0.9961	0.9969	0.9978
		B	0.9764	0.9888	0.9927	0.9945	0.9958	0.9967	0.9974	0.9980	0.9986
	16	A	0.9768	0.9882	0.9920	0.9946	0.9962	0.9973	0.9980	0.9989	0.9998
		B	0.9672	0.9805	0.9863	0.9899	0.9927	0.9952	0.9975	0.9991	1.0000

Model	# of machines	Seed	FPR@threshold								
			0.1	0.2	0.3	0.4	0.5	0.6	0.7	0.8	0.9
GAT	8	A	0.1327	0.0923	0.0732	0.0600	0.0494	0.0403	0.0312	0.0223	0.0095
		B	0.1396	0.0959	0.0754	0.0620	0.0514	0.0414	0.0322	0.0221	0.0093
	16	A	0.1350	0.0943	0.0735	0.0597	0.0477	0.0369	0.0266	0.0163	0.0039
		B	0.1208	0.0834	0.0642	0.0499	0.0372	0.0270	0.0171	0.0067	0.0005
GEM	8	A	0.0981	0.0560	0.0379	0.0271	0.0198	0.0141	0.0097	0.0055	0.0019
		B	0.0811	0.0461	0.0303	0.0213	0.0160	0.0118	0.0076	0.0041	0.0011
	16	A	0.1013	0.0589	0.0400	0.0284	0.0201	0.0130	0.0082	0.0037	0.0005
		B	0.0866	0.0503	0.0338	0.0241	0.0166	0.0110	0.0066	0.0027	0.0003
xFraud detector+	8	A	0.0279	0.0144	0.0098	0.0073	0.0059	0.0048	0.0039	0.0031	0.0022
		B	0.0236	0.0112	0.0073	0.0055	0.0042	0.0033	0.0026	0.0020	0.0014
	16	A	0.0232	0.0118	0.0080	0.0054	0.0038	0.0027	0.0020	0.0011	0.0002
		B	0.0328	0.0195	0.0137	0.0101	0.0073	0.0048	0.0025	0.0009	0.0000

Table 15: TPR, FNR, FPR, and TNR on *eBay-xlarge* by varying thresholds from 0.95 to 0.977 on the prediction scores.
FNR = 1 - TPR. The higher TPR is, the better; the lower FNR, the better.
FPR = 1 - TNR. The higher TNR is, the better; the lower FPR, the better.
"-" denotes that the scores do not exist for scores ⩾ threshold.

Model	# of machines	Seed	TPR@threshold									
			0.95	**0.96**	**0.97**	**0.971**	**0.972**	**0.973**	**0.974**	**0.975**	**0.976**	**0.977**
GAT	8	A	0.1820	0.1303	0.0717	0.0640	0.0595	0.0541	0.0471	0.0412	0.0362	0.0319
		B	0.1408	0.0903	0.0411	0.0363	0.0326	0.0285	0.0234	0.0188	0.0153	0.0123
	16	A	0.0380	0.0065	-	-	-	-	-	-	-	-
		B	0.0004	-	-	-	-	-	-	-	-	-
GEM	8	A	0.0699	0.0477	0.0192	0.0168	0.0142	0.0131	0.0113	0.0093	0.0080	0.0057
		B	0.0461	0.0171	0.0024	0.0020	0.0014	0.0014	0.0012	0.0010	0.0008	-
	16	A	0.0028	0.0008	-	-	-	-	-	-	-	-
		B	0.0006	-	-	-	-	-	-	-	-	-
xFraud detector+	8	A	0.3164	0.2930	0.2634	0.2548	0.2482	0.2401	0.2342	0.2255	0.2155	0.2063
		B	0.2714	0.2484	0.2024	0.1940	0.1867	0.1772	0.1663	0.1527	0.1381	0.1255
	16	A	0.0111	0.0014	-	-	-	-	-	-	-	-
		B	-	-	-	-	-	-	-	-	-	-

Model	# of machines	Seed	FNR@threshold									
			0.95	**0.96**	**0.97**	**0.971**	**0.972**	**0.973**	**0.974**	**0.975**	**0.976**	**0.977**
GAT	8	A	0.8180	0.8697	0.9283	0.9360	0.9405	0.9459	0.9529	0.9588	0.9638	0.9681
		B	0.8592	0.9097	0.9589	0.9637	0.9674	0.9715	0.9766	0.9812	0.9847	0.9877
	16	A	0.9620	0.9935	-	-	-	-	-	-	-	-
		B	0.9996	-	-	-	-	-	-	-	-	-
GEM	8	A	0.9301	0.9523	0.9808	0.9832	0.9858	0.9869	0.9887	0.9907	0.9920	0.9943
		B	0.9539	0.9829	0.9976	0.9980	0.9986	0.9986	0.9988	0.9990	0.9992	-
	16	A	0.9972	0.9992	-	-	-	-	-	-	-	-
		B	0.9994	-	-	-	-	-	-	-	-	-
xFraud detector+	8	A	0.6836	0.7070	0.7366	0.7452	0.7518	0.7599	0.7658	0.7745	0.7845	0.7937
		B	0.7286	0.7516	0.7976	0.8060	0.8133	0.8228	0.8337	0.8473	0.8619	0.8745
	16	A	0.9889	0.9986	-	-	-	-	-	-	-	-
		B	-	-	-	-	-	-	-	-	-	-

Model	# of machines	Seed	TNR@threshold									
			0.95	**0.96**	**0.97**	**0.971**	**0.972**	**0.973**	**0.974**	**0.975**	**0.976**	**0.977**
GAT	8	A	0.9977	0.9991	0.9998	0.9999	0.9999	0.9999	0.9999	0.9999	1.0000	1.0000
		B	0.9980	0.9992	0.9998	0.9998	0.9999	0.9999	0.9999	0.9999	1.0000	1.0000
	16	A	1.0000	1.0000	-	-	-	-	-	-	-	-
		B	1.0000	-	-	-	-	-	-	-	-	-
GEM	8	A	0.9996	0.9999	1.0000	1.0000	1.0000	1.0000	1.0000	1.0000	1.0000	1.0000
		B	0.9999	1.0000	1.0000	1.0000	1.0000	1.0000	1.0000	1.0000	1.0000	-
	16	A	1.0000	1.0000	-	-	-	-	-	-	-	-
		B	1.0000	-	-	-	-	-	-	-	-	-
xFraud detector+	8	A	0.9986	0.9989	0.9992	0.9992	0.9992	0.9993	0.9994	0.9994	0.9995	0.9995
		B	0.9991	0.9993	0.9996	0.9997	0.9998	0.9998	0.9998	0.9999	0.9999	0.9999
	16	A	1.0000	1.0000	-	-	-	-	-	-	-	-
		B	-	-	-	-	-	-	-	-	-	-

Model	# of machines	Seed	FPR@threshold									
			0.95	**0.96**	**0.97**	**0.971**	**0.972**	**0.973**	**0.974**	**0.975**	**0.976**	**0.977**
GAT	8	A	0.0023	0.0009	0.0002	0.0001	0.0001	0.0001	0.0001	0.0001	0.0000	0.0000
		B	0.0020	0.0008	0.0002	0.0002	0.0001	0.0001	0.0001	0.0001	0.0000	0.0000
	16	A	0.0000	0.0000	-	-	-	-	-	-	-	-
		B	0.0000	-	-	-	-	-	-	-	-	-
GEM	8	A	0.0004	0.0001	0.0000	0.0000	0.0000	0.0000	0.0000	0.0000	0.0000	0.0000
		B	0.0001	0.0000	0.0000	0.0000	0.0000	0.0000	0.0000	0.0000	0.0000	-
	16	A	0.0000	0.0000	-	-	-	-	-	-	-	-
		B	0.0000	-	-	-	-	-	-	-	-	-
xFraud detector+	8	A	0.0014	0.0011	0.0008	0.0008	0.0008	0.0007	0.0006	0.0006	0.0005	0.0005
		B	0.0009	0.0007	0.0004	0.0003	0.0002	0.0002	0.0002	0.0001	0.0001	0.0001
	16	A	0.0000	0.0000	-	-	-	-	-	-	-	-
		B	-	-	-	-	-	-	-	-	-	-

Table 16: TPR, FNR, FPR, and TNR on *eBay-xlarge* by varying thresholds from 0.978 to 0.987 on the prediction scores.
FNR = 1 - TPR. The higher TPR is, the better; the lower FNR, the better.
FPR = 1 - TNR. The higher TNR is, the better; the lower FPR, the better.
"-" denotes that the scores do not exist for scores ⩾ threshold.

Model	# of machines	Seed	TPR@threshold									
			0.978	**0.979**	**0.98**	**0.981**	**0.982**	**0.983**	**0.984**	**0.985**	**0.986**	**0.987**
GAT	8	A	0.0265	0.0181	0.0130	0.0088	0.0038	0.0008	0.0002	-	-	-
		B	0.0095	0.0056	0.0036	0.0028	0.0018	0.0006	-	-	-	
	16	A	-	-	-	-	-	-	-	-	-	-
		B	-	-	-	-	-	-	-	-	-	-
GEM	8	A	0.0045	0.0027	0.0018	0.0005	0.0005	0.0004	-	-	-	-
		B	-	-	-	-	-	-	-	-	-	-
	16	A	-	-	-	-	-	-	-	-	-	-
		B	-	-	-	-	-	-	-	-	-	-
xFraud detector+	8	A	0.1945	0.1820	0.1655	0.1504	0.1312	0.1091	0.0842	0.0623	0.0399	0.0196
		B	0.1102	0.0959	0.0823	0.0642	0.0443	0.0279	0.0099	0.0037	0.0010	0.0002
	16	A	-	-	-	-	-	-	-	-	-	-
		B	-	-	-	-	-	-	-	-	-	-

Model	# of machines	Seed	FNR@threshold									
			0.978	**0.979**	**0.98**	**0.981**	**0.982**	**0.983**	**0.984**	**0.985**	**0.986**	**0.987**
GAT	8	A	0.9735	0.9819	0.9870	0.9912	0.9962	0.9992	0.9998	-	-	-
		B	0.9905	0.9944	0.9964	0.9972	0.9982	0.9994		-	-	-
	16	A	-	-	-	-	-	-	-	-	-	-
		B	-	-	-	-	-	-	-	-	-	-
GEM	8	A	0.9955	0.9973	0.9982	0.9995	0.9995	0.9996	-	-	-	-
		B	-	-	-	-	-	-	-	-	-	-
	16	A	-	-	-	-	-	-	-	-	-	-
		B	-	-	-	-	-	-	-	-	-	-
xFraud detector+	8	A	0.8055	0.8180	0.8345	0.8496	0.8688	0.8909	0.9158	0.9377	0.9601	0.9804
		B	0.8898	0.9041	0.9177	0.9358	0.9557	0.9721	0.9901	0.9963	0.9990	0.9998
	16	A	-	-	-	-	-	-	-	-	-	-
		B	-	-	-	-	-	-	-	-	-	-

Model	# of machines	Seed	TNR@threshold									
			0.978	**0.979**	**0.98**	**0.981**	**0.982**	**0.983**	**0.984**	**0.985**	**0.986**	**0.987**
GAT	8	A	1.0000	1.0000	1.0000	1.0000	1.0000	1.0000	1.0000	-	-	-
		B	1.0000	1.0000	1.0000	1.0000	1.0000	1.0000	-	-	-	-
	16	A	-	-	-	-	-	-	-	-	-	-
		B	-	-	-	-	-	-	-	-	-	-
GEM	8	A	1.0000	1.0000	1.0000	1.0000	1.0000	1.0000	-	-	-	-
		B	-	-	-	-	-	-	-	-	-	-
	16	A	-	-	-	-	-	-	-	-	-	-
		B	-	-	-	-	-	-	-	-	-	-
xFraud detector+	8	A	0.9996	0.9996	0.9997	0.9997	0.9999	0.9999	1.0000	1.0000	1.0000	1.0000
		B	1.0000	1.0000	1.0000	1.0000	1.0000	1.0000	1.0000	1.0000	1.0000	1.0000
	16	A	-	-	-	-	-	-	-	-	-	-
		B	-	-	-	-	-	-	-	-	-	-

Model	# of machines	Seed	FPR@threshold									
			0.978	**0.979**	**0.98**	**0.981**	**0.982**	**0.983**	**0.984**	**0.985**	**0.986**	**0.987**
GAT	8	A	0.0000	0.0000	0.0000	0.0000	0.0000	0.0000	0.0000	-	-	-
		B	0.0000	0.0000	0.0000	0.0000	0.0000	0.0000	-	-	-	-
	16	A	-	-	-	-	-	-	-	-	-	-
		B	-	-	-	-	-	-	-	-	-	-
GEM	8	A	0.0000	0.0000	0.0000	0.0000	0.0000	0.0000	-	-	-	-
		B	-	-	-	-	-	-	-	-	-	-
	16	A	-	-	-	-	-	-	-	-	-	-
		B	-	-	-	-	-	-	-	-	-	-
xFraud detector+	8	A	0.0004	0.0004	0.0003	0.0003	0.0001	0.0001	0.0000	0.0000	0.0000	0.0000
		B	0.0000	0.0000	0.0000	0.0000	0.0000	0.0000	0.0000	0.0000	0.0000	0.0000
	16	A	-	-	-	-	-	-	-	-	-	-
		B	-	-	-	-	-	-	-	-	-	-

Table 17: Precision and recall on *eBay-xlarge* by varying thresholds from 0.1 to 0.9 on the prediction scores.

Model	# of machines	Seed	Precision@threshold								
			0.1	**0.2**	**0.3**	**0.4**	**0.5**	**0.6**	**0.7**	**0.8**	**0.9**
GAT	8	A	0.2010	0.2478	0.2792	0.3074	0.3362	0.3666	0.4071	0.4592	0.6021
		B	0.1943	0.2391	0.2706	0.2968	0.3219	0.3544	0.3917	0.4488	0.5755
	16	A	0.1996	0.2456	0.2797	0.3098	0.3420	0.3852	0.4397	0.5124	0.7124
		B	0.2109	0.2542	0.2916	0.3285	0.3750	0.4217	0.4796	0.6028	0.8057
GEM	8	A	0.2472	0.3276	0.3822	0.4351	0.4812	0.5329	0.5908	0.6741	0.7904
		B	0.2731	0.3553	0.4231	0.4814	0.5175	0.5618	0.6321	0.7213	0.8509
	16	A	0.2395	0.3178	0.3729	0.4228	0.4788	0.5488	0.6133	0.7118	0.8525
		B	0.2579	0.3369	0.3985	0.4481	0.5105	0.5737	0.6352	0.7460	0.9040
xFraud detector+	8	A	0.4820	0.6144	0.6894	0.7383	0.7713	0.8025	0.8249	0.8529	0.8798
		B	0.5122	0.6588	0.7346	0.7771	0.8157	0.8409	0.8660	0.8924	0.9119
	16	A	0.4960	0.6345	0.7030	0.7679	0.8188	0.8552	0.8791	0.9223	0.9689
		B	0.4179	0.5133	0.5805	0.6363	0.6871	0.7466	0.8188	0.8939	0.8846
Model	**# of machines**	**Seed**	**Recall@threshold**								
			0.1	**0.2**	**0.3**	**0.4**	**0.5**	**0.6**	**0.7**	**0.8**	**0.9**
GAT	8	A	0.7379	0.6718	0.6264	0.5891	0.5535	0.5158	0.4730	0.4187	0.3170
		B	0.7443	0.6664	0.6184	0.5787	0.5391	0.5030	0.4577	0.3972	0.2780
	16	A	0.7439	0.6789	0.6311	0.5923	0.5483	0.5112	0.4614	0.3790	0.2152
		B	0.7137	0.6287	0.5839	0.5396	0.4930	0.4345	0.3488	0.2262	0.0432
GEM	8	A	0.7125	0.6028	0.5182	0.4608	0.4058	0.3563	0.3086	0.2501	0.1599
		B	0.6737	0.5611	0.4913	0.4363	0.3788	0.3349	0.2902	0.2344	0.1360
	16	A	0.7052	0.6061	0.5263	0.4592	0.4073	0.3490	0.2859	0.2014	0.0660
		B	0.6649	0.5646	0.4955	0.4331	0.3829	0.3282	0.2522	0.1742	0.0588
xFraud detector+	8	A	0.5731	0.5083	0.4794	0.4582	0.4407	0.4268	0.4103	0.3933	0.3621
		B	0.5480	0.4801	0.4482	0.4213	0.4067	0.3904	0.3746	0.3579	0.3199
	16	A	0.5056	0.4521	0.4198	0.3978	0.3757	0.3526	0.3228	0.2794	0.1424
		B	0.5212	0.4549	0.4177	0.3902	0.3524	0.3113	0.2529	0.1597	0.0018

Table 18: Precision and recall on *eBay-xlarge* by varying thresholds from 0.95 to 0.977 on the prediction scores. "-" denotes that the scores do not exist for scores ⩾ threshold.

Model	# of machines	Seed	Precision@threshold									
			0.95	**0.96**	**0.97**	**0.971**	**0.972**	**0.973**	**0.974**	**0.975**	**0.976**	**0.977**
GAT	8	A	0.7832	0.8682	0.9392	0.9568	0.9606	0.9634	0.9642	0.9661	0.9814	0.9882
		B	0.7647	0.8358	0.9000	0.9034	0.9224	0.9144	0.9331	0.9251	0.9481	0.9759
	16	A	0.9784	1.0000	-	-	-	-	-	-	-	-
		B	1.0000	-	-	-	-	-	-	-	-	-
GEM	8	A	0.8930	0.9372	0.9655	0.9607	0.9541	0.9503	0.9430	0.9313	0.9813	1.0000
		B	0.9712	1.0000	1.0000	1.0000	1.0000	1.0000	1.0000	1.0000	1.0000	-
	16	A	0.9024	1.0000	-	-	-	-	-	-	-	-
		B	1.0000	-	-	-	-	-	-	-	-	-
xFraud detector+	8	A	0.9106	0.9217	0.9359	0.9370	0.9373	0.9412	0.9436	0.9433	0.9500	0.9539
		B	0.9313	0.9392	0.9613	0.9637	0.9722	0.9736	0.9785	0.9795	0.9837	0.9868
	16	A	0.9733	1.0000	-	-	-	-	-	-	-	-
		B	-	-	-	-	-	-	-	-	-	-

Model	# of machines	Seed	Recall@threshold									
			0.95	**0.96**	**0.97**	**0.971**	**0.972**	**0.973**	**0.974**	**0.975**	**0.976**	**0.977**
GAT	8	A	0.1820	0.1303	0.0717	0.0640	0.0595	0.0541	0.0471	0.0412	0.0362	0.0319
		B	0.1408	0.0903	0.0411	0.0363	0.0326	0.0285	0.0234	0.0188	0.0153	0.0123
	16	A	0.0380	0.0065	-	-	-	-	-	-	-	-
		B	0.0004	-	-	-	-	-	-	-	-	-
GEM	8	A	0.0699	0.0477	0.0192	0.0168	0.0142	0.0131	0.0113	0.0093	0.0080	0.0057
		B	0.0461	0.0171	0.0024	0.0020	0.0014	0.0014	0.0012	0.0010	0.0008	-
	16	A	0.0028	0.0008	-	-	-	-	-	-	-	-
		B	0.0006	-	-	-	-	-	-	-	-	-
xFraud detector+	8	A	0.3164	0.2930	0.2634	0.2548	0.2482	0.2401	0.2342	0.2255	0.2155	0.2063
		B	0.2714	0.2484	0.2024	0.1940	0.1867	0.1772	0.1663	0.1527	0.1381	0.1255
	16	A	0.0111	0.0014	-	-	-	-	-	-	-	-
		B	-	-	-	-	-	-	-	-	-	-

Table 19: Precision and recall on *eBay-xlarge* by varying thresholds from 0.978 to 0.987 on the prediction scores. "-" denotes that the scores do not exist for scores ⩾ threshold.

Model	# of machines	Seed	Precision@threshold									
			0.978	**0.979**	**0.98**	**0.981**	**0.982**	**0.983**	**0.984**	**0.985**	**0.986**	**0.987**
GAT	8	A	0.9971	0.9958	0.9942	1.0000	1.0000	1.0000	1.0000	-	-	-
		B	0.9690	0.9487	0.9216	0.9024	0.8519	0.6667	-	-	-	-
	16	A	-	-	-	-	-	-	-	-	-	-
		B	-	-	-	-	-	-	-	-	-	-
GEM	8	A	1.0000	1.0000	1.0000	1.0000	1.0000	1.0000	-	-	-	-
		B	-	-	-	-	-	-	-	-	-	-
	16	A	-	-	-	-	-	-	-	-	-	-
		B	-	-	-	-	-	-	-	-	-	-
xFraud detector+	8	A	0.9537	0.9545	0.9586	0.9625	0.9829	0.9822	0.9910	0.9879	0.9905	0.9809
		B	0.9918	0.9906	0.9982	0.9976	0.9966	1.0000	1.0000	1.0000	1.0000	1.0000
	16	A	-	-	-	-	-	-	-	-	-	-
		B	-	-	-	-	-	-	-	-	-	-
Model	**# of machines**	**Seed**	**Recall@threshold**									
			0.978	**0.979**	**0.98**	**0.981**	**0.982**	**0.983**	**0.984**	**0.985**	**0.986**	**0.987**
GAT	8	A	0.0265	0.0181	0.0130	0.0088	0.0038	0.0008	0.0002	-	-	-
		B	0.0095	0.0056	0.0036	0.0028	0.0018	0.0006	-	-	-	-
	16	A	-	-	-	-	-	-	-	-	-	-
		B	-	-	-	-	-	-	-	-	-	-
GEM	8	A	0.0045	0.0027	0.0018	0.0005	0.0005	0.0004	-	-	-	-
		B	-	-	-	-	-	-	-	-	-	-
16	A	-	-	-	-	-	-	-	-	-	-	
		B	-	-	-	-	-	-	-	-	-	-
xFraud detector+	8	A	0.1945	0.1820	0.1655	0.1504	0.1312	0.1091	0.0842	0.0623	0.0399	0.0196
		B	0.1102	0.0959	0.0823	0.0642	0.0443	0.0279	0.0099	0.0037	0.0010	0.0002
	16	A	-	-	-	-	-	-	-	-	-	-
		B	-	-	-	-	-	-	-	-	-	-

REFERENCES

[1] Bart Baesens, Veronique Van Vlasselaer, and Wouter Verbeke. 2015. *Fraud analytics using descriptive, predictive, and social network techniques: a guide to data science for fraud detection.* John Wiley & Sons.

[2] Federico Baldassarre and Hossein Azizpour. 2019. Explainability techniques for graph convolutional networks. *arXiv preprint arXiv:1905.13686* (2019).

[3] Adam Breuer, Roee Eilat, and Udi Weinsberg. 2020. Friend or Faux: Graph-Based Early Detection of Fake Accounts on Social Networks. In *Proceedings of The Web Conference 2020.* 1287–1297.

[4] Bokai Cao, Mia Mao, Siim Viidu, and S Yu Philip. 2017. HitFraud: a broad learning approach for collective fraud detection in heterogeneous information networks. In *2017 IEEE international conference on data mining (ICDM).* IEEE, 769–774.

[5] Shaosheng Cao, XinXing Yang, Cen Chen, Jun Zhou, Xiaolong Li, and Yuan Qi. 2019. TitAnt: online real-time transaction fraud detection in Ant Financial. *Proceedings of the VLDB Endowment* (2019).

[6] Yukuo Cen, Xu Zou, Jianwei Zhang, Hongxia Yang, Jingren Zhou, and Jie Tang. 2019. Representation learning for attributed multiplex heterogeneous network. In *Proceedings of the 25th ACM SIGKDD International Conference on Knowledge Discovery & Data Mining.* 1358–1368.

[7] Shiyu Chang, Wei Han, Jiliang Tang, Guo-Jun Qi, Charu C Aggarwal, and Thomas S Huang. 2015. Heterogeneous network embedding via deep architectures. In *Proceedings of the 21th ACM SIGKDD international conference on knowledge discovery and data mining.* 119–128.

[8] Sarthika Dhawan, Siva Charan Reddy Gangireddy, Shiv Kumar, and Tanmoy Chakraborty. 2019. Spotting collective behaviour of online frauds in customer reviews. *arXiv preprint arXiv:1905.13649* (2019).

[9] Yuxiao Dong, Nitesh V Chawla, and Ananthram Swami. 2017. metapath2vec: Scalable representation learning for heterogeneous networks. In *Proceedings of the 23rd ACM SIGKDD international conference on knowledge discovery and data mining.* 135–144.

[10] Paul Emmerich, Maximilian Pudelko, Sebastian Gallenmüller, and Georg Carle. 2017. FlowScope: Efficient packet capture and storage in 100 Gbit/s networks. In *2017 IFIP Networking Conference (IFIP Networking) and Workshops.* IEEE, 1–9.

[11] Dhivya Eswaran, Stephan Günnemann, Christos Faloutsos, Disha Makhija, and Mohit Kumar. 2017. Zoobp: Belief propagation for heterogeneous networks. *Proceedings of the VLDB Endowment* 10, 5 (2017), 625–636.

[12] V. Fomin, J. Anmol, S. Desroziers, J. Kriss, and A. Tejani. 2020. High-level library to help with training neural networks in PyTorch. https://github.com/pytorch/ignite.

[13] Xinyu Fu, Jiani Zhang, Ziqiao Meng, and Irwin King. 2020. Magnn: Metapath aggregated graph neural network for heterogeneous graph embedding. In *Proceedings of The Web Conference 2020.* 2331–2341.

[14] Will Hamilton, Zhitao Ying, and Jure Leskovec. 2017. Inductive representation learning on large graphs. In *Advances in neural information processing systems.* 1024–1034.

[15] Bryan Hooi, Hyun Ah Song, Alex Beutel, Neil Shah, Kijung Shin, and Christos Faloutsos. 2016. Fraudar: Bounding graph fraud in the face of camouflage. In *Proceedings of the 22nd ACM SIGKDD International Conference on Knowledge Discovery and Data Mining.* 895–904.

[16] Binbin Hu, Yuan Fang, and Chuan Shi. 2019. Adversarial learning on heterogeneous information networks. In *Proceedings of the 25th ACM SIGKDD International Conference on Knowledge Discovery & Data Mining.* 120–129.

[17] Binbin Hu, Zhiqiang Zhang, Chuan Shi, Jun Zhou, Xiaolong Li, and Yuan Qi. 2019. Cash-out user detection based on attributed heterogeneous information network with a hierarchical attention mechanism. In *Proceedings of the AAAI Conference on Artificial Intelligence*, Vol. 33. 946–953.

[18] Ziniu Hu, Yuxiao Dong, Kuansan Wang, and Yizhou Sun. 2020. Heterogeneous graph transformer. In *Proceedings of The Web Conference 2020.* 2704–2710.

[19] Qiang Huang, Makoto Yamada, Yuan Tian, Dinesh Singh, Dawei Yin, and Yi Chang. 2020. GraphLIME: Local interpretable model explanations for graph neural networks. *arXiv preprint arXiv:2001.06216* (2020).

[20] Parisa Kaghazgaran, James Caverlee, and Anna Squicciarini. 2018. Combating crowdsourced review manipulators: A neighborhood-based approach. In *Proceedings of the Eleventh ACM International Conference on Web Search and Data Mining.* 306–314.

[21] Srijan Kumar, Bryan Hooi, Disha Makhija, Mohit Kumar, Christos Faloutsos, and VS Subrahmanian. 2018. Rev2: Fraudulent user prediction in rating platforms. In *Proceedings of the Eleventh ACM International Conference on Web Search and Data Mining.* 333–341.

[22] Ao Li, Zhou Qin, Runshi Liu, Yiqun Yang, and Dong Li. 2019. Spam review detection with graph convolutional networks. In *Proceedings of the 28th ACM International Conference on Information and Knowledge Management.* 2703–2711.

[23] Xiang Li, Wen Zhang, Jiuzhou Xi, and Hao Zhu. 2018. HGsuspector: Scalable Collective Fraud Detection in Heterogeneous Graphs. (2018).

[24] Chen Liang, Ziqi Liu, Bin Liu, Jun Zhou, Xiaolong Li, Shuang Yang, and Yuan Qi. 2019. Uncovering Insurance Fraud Conspiracy with Network Learning. In *Proceedings of the 42nd International ACM SIGIR Conference on Research and Development in Information Retrieval.* 1181–1184.

[25] Frank Lin and William W Cohen. 2010. Power iteration clustering. In *ICML.*

[26] Shenghua Liu, Bryan Hooi, and Christos Faloutsos. 2017. Holoscope: Topology-and-spike aware fraud detection. In *Proceedings of the 2017 ACM on Conference on Information and Knowledge Management.* 1539–1548.

[27] Ziqi Liu, Chaochao Chen, Longfei Li, Jun Zhou, Xiaolong Li, Le Song, and Yuan Qi. 2019. Geniepath: Graph neural networks with adaptive receptive paths. In *Proceedings of the AAAI Conference on Artificial Intelligence*, Vol. 33. 4424–4431.

[28] Ziqi Liu, Chaochao Chen, Xinxing Yang, Jun Zhou, Xiaolong Li, and Le Song. 2018. Heterogeneous graph neural networks for malicious account detection. In *Proceedings of the 27th ACM International Conference on Information and Knowledge Management.* 2077–2085.

[29] Zhiwei Liu, Yingtong Dou, Philip S Yu, Yutong Deng, and Hao Peng. 2020. Alleviating the Inconsistency Problem of Applying Graph Neural Network to Fraud Detection. *arXiv preprint arXiv:2005.00625* (2020).

[30] Qingsong Lv, Ming Ding, Qiang Liu, Yuxiang Chen, Wenzheng Feng, Siming He, Chang Zhou, Jianguo Jiang, Yuxiao Dong, and Jie Tang. 2021. Are we really making much progress? Revisiting, benchmarking, and refining heterogeneous graph neural networks. (2021).

[31] Jun Ma, Danqing Zhang, Yun Wang, Yan Zhang, and Alexey Pozdnoukhov. 2018. GraphRAD: A Graph-based Risky Account Detection System. (2018).

[32] Wei Min, Zhengyang Tang, Min Zhu, Yuxi Dai, Yan Wei, and Ruinan Zhang. 2018. Behavior language processing with graph based feature generation for fraud detection in online lending. In *Proceedings of Workshop on Misinformation and Misbehavior Mining on the Web.*

[33] Hamed Nilforoshan and Neil Shah. 2019. SliceNDice: Mining Suspicious Multi-Attribute Entity Groups with Multi-View Graphs. In *2019 IEEE International Conference on Data Science and Advanced Analytics (DSAA).* IEEE, 351–363.

[34] Susie Xi Rao, Shuai Zhang, Zhichao Han, Zitao Zhang, Wei Min, Zhiyao Chen, Yinan Shan, Yang Zhao, and Ce Zhang. 2021. Appendix for xFraud: Explainable Fraud Transaction Detection. https://github.com/eBay/xFraud/blob/master/documents/Appendix_XFraud_VLDB.pdf.

[35] Yuxiang Ren, Hao Zhu, Jiawei ZHang, Peng Dai, and Liefeng Bo. 2019. EnsemFDet: An Ensemble Approach to Fraud Detection based on Bipartite Graph. *arXiv preprint arXiv:1912.11113* (2019).

[36] Chuan Shi, Binbin Hu, Wayne Xin Zhao, and S Yu Philip. 2018. Heterogeneous information network embedding for recommendation. *IEEE Transactions on Knowledge and Data Engineering* 31, 2 (2018), 357–370.

[37] Yu Shi, Fangqiu Han, Xinwei He, Xinran He, Carl Yang, Jie Luo, and Jiawei Han. 2018. mvn2vec: Preservation and collaboration in multi-view network embedding. *arXiv preprint arXiv:1801.06597* (2018).

[38] Kai Shu, Deepak Mahudeswaran, Suhang Wang, and Huan Liu. 2020. Hierarchical propagation networks for fake news detection: Investigation and exploitation. In *Proceedings of the International AAAI Conference on Web and Social Media*, Vol. 14. 626–637.

[39] Ashish Vaswani, Noam Shazeer, Niki Parmar, Jakob Uszkoreit, Llion Jones, Aidan N Gomez, Łukasz Kaiser, and Illia Polosukhin. 2017. Attention is all you need. In *Advances in neural information processing systems.* 5998–6008.

[40] Haibo Wang, Chuan Zhou, Jia Wu, Weizhen Dang, Xingquan Zhu, and Jilong Wang. 2018. Deep structure learning for fraud detection. In *2018 IEEE International Conference on Data Mining (ICDM).* IEEE, 567–576.

[41] Jianyu Wang, Rui Wen, Chunming Wu, Yu Huang, and Jian Xion. 2019. Fdgars: Fraudster detection via graph convolutional networks in online app review system. In *Companion Proceedings of The 2019 World Wide Web Conference.* 310–316.

[42] Xiao Wang, Houye Ji, Chuan Shi, Bai Wang, Yanfang Ye, Peng Cui, and Philip S Yu. 2019. Heterogeneous graph attention network. In *The World Wide Web Conference.* 2022–2032.

[43] Mark Weber, Giacomo Domeniconi, Jie Chen, Daniel Karl I Weidele, Claudio Bellei, Tom Robinson, and Charles E Leiserson. 2019. Anti-money laundering in bitcoin: Experimenting with graph convolutional networks for financial forensics. *arXiv preprint arXiv:1908.02591* (2019).

[44] Rui Wen, Jianyu Wang, Chunming Wu, and Jian Xiong. 2020. ASA: Adversary Situation Awareness via Heterogeneous Graph Convolutional Networks. In *Companion Proceedings of the Web Conference 2020.* 674–678.

[45] P. Reddy X. Li, J. Saude and M. Veloso. 2020. Classifying and understanding financial data using graph neural network. In *AAAI.*

[46] Carl Yang, Yuxin Xiao, Yu Zhang, Yizhou Sun, and Jiawei Han. 2020. Heterogeneous network representation learning: A unified framework with survey and benchmark. *IEEE Transactions on Knowledge and Data Engineering* (2020).

[47] Zhitao Ying, Dylan Bourgeois, Jiaxuan You, Marinka Zitnik, and Jure Leskovec. 2019. Gnnexplainer: Generating explanations for graph neural networks. In *Advances in neural information processing systems.* 9244–9255.

[48] Hao Yuan, Jiliang Tang, Xia Hu, and Shuiwang Ji. 2020. XGNN: Towards Model-Level Explanations of Graph Neural Networks. *arXiv preprint arXiv:2006.02587* (2020).

[49] Seongjun Yun, Minbyul Jeong, Raehyun Kim, Jaewoo Kang, and Hyunwoo J Kim. 2019. Graph transformer networks. *Advances in Neural Information Processing Systems* 32 (2019), 11983–11993.

[50] Chuxu Zhang, Dongjin Song, Chao Huang, Ananthram Swami, and Nitesh V Chawla. 2019. Heterogeneous graph neural network. In *Proceedings of the 25th ACM SIGKDD International Conference on Knowledge Discovery & Data Mining*. 793–803.

[51] Yiming Zhang, Yujie Fan, Yanfang Ye, Liang Zhao, and Chuan Shi. 2019. Key Player Identification in Underground Forums over Attributed Heterogeneous Information Network Embedding Framework. In *Proceedings of the 28th ACM International Conference on Information and Knowledge Management*. 549–558.

[52] Kai Zhao, Ting Bai, Bin Wu, Bai Wang, Youjie Zhang, Yuanyu Yang, and Jian-Yun Nie. 2020. Deep adversarial completion for sparse heterogeneous information network embedding. In *Proceedings of the Web Conference 2020*. 508–518.

[53] Qiwei Zhong, Yang Liu, Xiang Ao, Binbin Hu, Jinghua Feng, Jiayu Tang, and Qing He. 2020. Financial Defaulter Detection on Online Credit Payment via Multi-view Attributed Heterogeneous Information Network. In *Proceedings of The Web Conference 2020*. 785–795.

[54] Yongchun Zhu, Dongbo Xi, Bowen Song, Fuzhen Zhuang, Shuai Chen, Xi Gu, and Qing He. 2020. Modeling Users' Behavior Sequences with Hierarchical Explainable Network for Cross-domain Fraud Detection. In *Proceedings of The Web Conference 2020*. 928–938.